Pergamon

Cement and Concrete Research 29 (1999) 631–633

CEMENT AND CONCRETE RESEARCH

Communication

Pore structure and its effect on strength of high-volume fly ash paste

Linhua Jiang *, Yugang Guan

College of Civil Engineering, Hohai University, Nanjing 210098, People's Republic of China

Manuscript received 8 December 1998; accepted manuscript 5 February 1999

Abstract

Pastes made with different fly ash contents and water/binder ratios were tested at different ages. The total porosity and pore size distribution were measured by mercury intrusion. The fractal dimension of pore-solid interface was first measured by small angle X-ray scattering (SAXS). The relationship between porosity and strength for high-volume fly ash (HVFA) paste was determined. It is obtained that the pore size distribution affected both compressive strength and flexural strength, but the effects on compressive strength and on flexural strength are different. Preliminary experimental results indicated that strength was closely related to the pore surface fractal dimension.

Keywords: Mercury porosimetry; Small-angle X-ray scattering; Bending strength; Compressive strength; Fly ash

The study of pore structure of Portland cement paste has considerable value in efforts to understand the nature of this complex material [1]. The relationship between total porosity and strength has been extensively studied. The effects of other factors on strength such as pore size distribution and specific surface area have also been studied. It has by now been ascertained that there is a close relationship between total porosity, pore size distribution, and strength [1,2]. However, there has been little information available concerning high-volume fly ash (HVFA) paste, especially with reference to the fractal dimension of pore-solid interface and the effect of pore structure on flexural strength. The purpose of this work was to investigate the pore structure and its effect on strength of HVFA paste.

1. Experimental

1.1. Materials

The cement used in all mixes was Portland cement. The fly ash, obtained from Chongqing, China, was a Class I type (Chinese standard). The chemical analyses and physical properties of the cement and fly ash are presented in Table 1. The admixtures used in this study were water-reducing admixture (SA-1) and excitant admixture (SA-2).

1.2. Paste mixtures and specimens

Paste mixtures of different fly ash contents and water/binder ratios were prepared. The nomenclature used for these five mixes is presented in Table 2. The consistency of each mix is standard consistency, except for mix F552. The $40 \times 40 \times 160$-mm prisms were prepared for strength measurements and 40-mm cubes were prepared for pore structure measurements.

1.3. Tests

Total porosity and pore size distribution were carried out using an Outoscan mercury intrusion porosimeter. Strength was measured according to GB177-85 (Chinese standard). The specimens were first tested in flexure, then in compression. Fractal dimension of pore-solid interface was measured by small angle X-ray scattering (SAXS) [1,3].

2. Results and discussion

2.1. Total porosity

Total porosity obtained by mercury intrusion is presented in Table 3. The total porosity increased with increasing fly ash content and water/binder ratio and decreased with increasing curing age.

2.2. Pore size distribution

The results of the mercury intrusion for the five mixtures were obtained at hydration times of 3, 28, or 90 days, and

* Corresponding author's present address is Materials Technology Laboratory, CANMET, 405 Rochester Street, Ottawa, Ontario, K1A 0G1 Canada. Tel.: 613-992-5346; Fax: 613-992-9389; E-mail: ljiang@nrcan.gc.ca.

0008-8846/99/$–see front matter
PII: S0008-8846(99)00034-4

Table 1
Composition (mass %) and physical properties of portland cement and fly ash

	Portland cement	Fly ash
SiO_2	21.42	44.98
Al_2O_3	4.68	30.08
Fe_2O_3	6.15	13.92
CaO	63.78	3.69
MgO	1.88	1.41
SO_3	1.08	0.15
Na_2O	0.19	—
K_2O	0.53	—
Loss on ignition	1.55	4.34
Specific gravity	3.16	2.38
Fineness, retained on a 45 μm sieve (%)	8.5	2.3

Table 3
Total porosity of the pastes (%)

Nomenclature	3 days	28 days	90 days
C0	22.91	17.90	15.56
F40	—	25.23	—
F551	32.22	27.68	25.14
F70	—	36.32	—
F552	—	33.39	—

show the development of pore structure. Figs. 1 and 2 report the pore size distribution for the neat cement C0 and HVFA pastes F551 at 3, 28, and 90 days, respectively. It is obvious that the pores of higher size decreased with increasing age for both mixtures. The pores with radii $r < 20$ nm increased more in HVFA paste than in neat cement paste.

2.3. Strength

The results of compressive and flexural strength at different curing ages are given in Table 4. It can be seen that the early strength of HVFA pastes is lower than that of neat cement pastes, but the later strength of HVFA pastes increases more than that of neat cement pastes.

2.4. Pore surface fractal dimension

The results of fractal dimension of pore-solid interface measured by SAXS are shown in Table 5. Pore surface fractal dimension increased with increasing fly ash content and water/binder ratio.

2.5. Relationship between compressive strength and total porosity

By linear regression, the linear correlation between total porosity and strength for HVFA pastes was observed. The equations for strength-porosity relationships were $\sigma_c = 127.04\text{-}2.93P$ and $\sigma_f = 10.29\text{-}0.20P$. Where σ_c,σ_f are compressive strength and flexural strength, respectively; P is the porosity (in percent).

Table 2
Nomenclature for cement and cement fly ash mixtures

Nomenclature	F/(C + F) (%)	W/(C + F)	Admixture (%)
C0	0	0.26	—
F40	40	0.27	SA-1, 1.7;SA-2, 0.8
F551	55	0.28	SA-1, 1.7;SA-2, 0.8
F70	70	0.30	SA-1, 1.7;SA-2, 0.8
F552	55	0.38	SA-1, 1.7;SA-2, 0.8

2.6. Effect of pore size distribution on strength of HVFA pastes

To analyze the effect of pores of different radii on compressive strength, the multiple linear regression analysis was carried out. The following equation was obtained:

$$\sigma_c = 93.53 - 0.05P_{<20} - 3.30P_{20\text{–}50} - 0.71P_{50\text{–}100} - 10.87P_{>100} \quad (1)$$

where $P_{<20}$, $P_{20\text{–}50}$, $P_{50\text{–}100}$, and $P_{>100}$ are the volumes (in percent) of pores with radii $r < 20$ nm, $r = 20\text{–}50$ nm, $r = 50\text{–}100$ nm, and $r > 100$ nm, respectively. The obtained results [Eq. (1)] indicated different effects of pores with different radii on the strength of HVFA pastes: The presence of very small pores with radii $r < 20$ nm appears to lower the strength only insignificantly, while the effect of those with radii $r > 100$ nm is distinctly higher. It may be noted, however, that the effect of the pores with radii $r = 20\text{–}50$ nm is higher than that of those with radii $r = 50\text{–}100$ nm. By scanning electron microscope examination, it is discovered that some of the pores with radii $r = 20\text{–}50$ nm may be the interfacial cracks around some fly ash particles.

The multiple linear regression analysis for flexural strength was also carried out. The equation obtained is:

$$\sigma_f = 11.60 - 0.08P_{<20} - 0.36P_{20\text{–}50} - 0.21P_{50\text{–}100} - 0.45P_{>100} \quad (2)$$

Eq. (2) shows that the effects of pore size distribution on flexural strength and on compressive strength are different. All the pores with different radii have an effect on flexural strength.

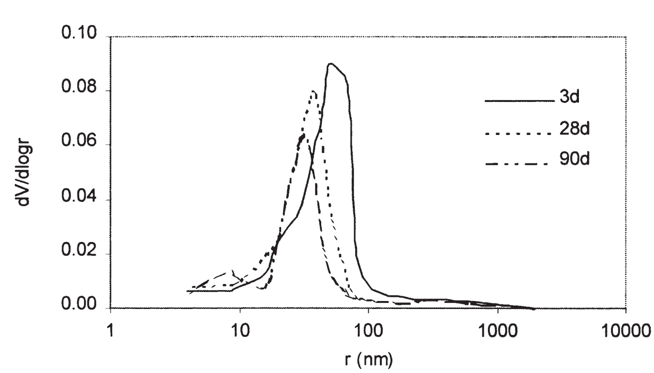

Fig. 1. Pore size distribution for mixture C0.

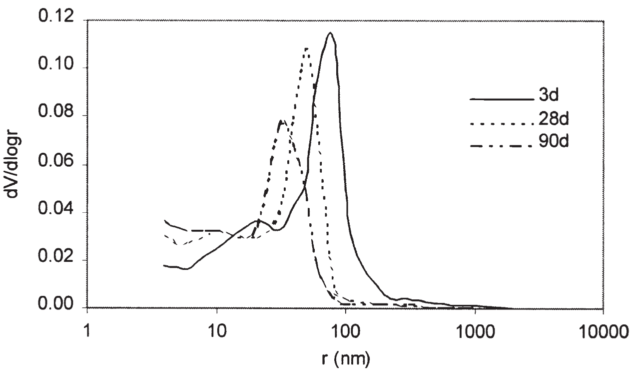

Fig. 2. Pore size distribution for mixture F551.

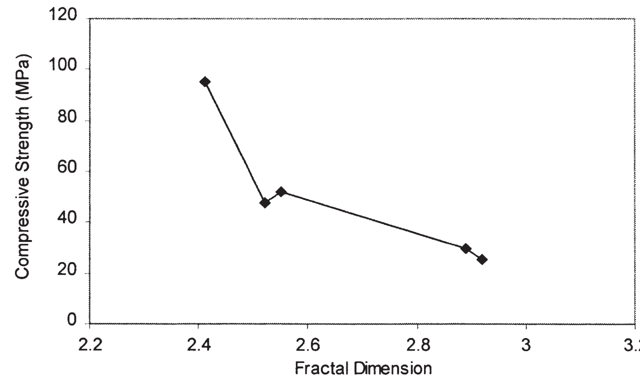

Fig. 3. The strength vs. fractal dimension relation.

2.7. Relationship between strength and pore surface fractal dimension

The preliminary results about the relationship between compressive strength and pore surface fractal dimension are shown in Fig. 3. The compressive strength decreased with increasing fractal dimension. Because of only a few data obtained, the quantitative relationship between compressive strength and fractal dimension was not determined. To obtain the quantitative relationship between strength and fractal dimension, more test results are needed.

3. Conclusions

Based on the above results and discussion, the following conclusions can be drawn:

- The total porosity of the paste increased with increasing fly ash content and water/binder ratio and decreased with increasing age.
- The pore size distribution of HVFA paste is different from that of neat cement paste.
- For HVFA paste, the linear relationship similar to that for neat cement paste exists between total porosity and compressive strength; the linear relationship between total porosity and flexural strength also exists.
- The effects of pore size distribution on compressive strength and on flexural strength are different. The porosity located in pores with radii $r < 20$ nm only negligibly affects compressive strength. The effect of porosity located in pores with radii $r > 100$ nm is distinctly greater than of those located in pores with other radii. For flexural strength, all the pores affect strength.

The preliminary test results show that the strength increased with decreasing pore surface fractal dimension. To obtain the quantitative relationship between the strength and fractal dimension, further investigation is needed.

References

[1] L.H. Jiang, Hydration, Microstructure and Mechanism of High Volume Fly Ash Concrete. PhD dissertation, Hohai University, Nanjing, 1998.

[2] Y.G. Guan, Strength Mechanism of the HVFA Cement Paste and Concrete. Master thesis, Hohai University, Nanjing, 1998.

[3] H.D. Bale and P.W. Schmitdt, Small-angle x-ray-scatting investigation of submicroscopic porosity with fractal properties, J Phys Rev Lett 53 (1984) 596–599.

Table 4
Compressive strength and flexural strength of the pastes (MPa)

	Compressive strength				Flexural strength			
Nomenclature	3 days	7 days	28 days	90 days	3 days	7 days	28 days	90 days
CO	63.0	68.8	95.3	96.4	12.2	14.4	12.9	12.9
F40	28.6	36.0	47.5	74.4	5.6	6.2	5.2	7.3
F551	20.6	27.0	52.1	59.8	3.8	4.5	5.1	5.8
F70	14.5	20.0	29.9	48.8	2.6	3.1	3.8	4.5
F552	0.9	13.2	25.4	57.2	0.3	3.1	3.3	4.6

Table 5
Pore surface fractal dimension of the pastes

Nomenclature	C0	F40	F551	F70	F552
D_s*	2.41 ± 0.07	2.52 ± 0.05	2.55 ± 0.06	2.89 ± 0.06	2.92 ± 0.05

*D_s is pore surface fractal dimension.